One- and Two-Dimensional Wind Speed Models for Ka-Band Altimetry

JOHN LILLIBRIDGE

National Oceanic and Atmospheric Administration/Laboratory for Satellite Altimetry, College Park, Maryland

REMKO SCHARROO

European Organisation for the Exploitation of Meteorological Satellites, Darmstadt, Germany

SALEH ABDALLA

European Centre for Medium-Range Weather Forecasting, Reading, United Kingdom

DOUG VANDEMARK

University of New Hampshire, Durham, New Hampshire

(Manuscript received 5 August 2013, in final form 22 October 2013)

ABSTRACT

SARAL—the Satellite with ARgos and ALtiKa—is the first satellite radar altimetry mission to fly a Ka-band instrument (AltiKa). Ocean backscatter measurements in the Ka band suffer larger signal attenuation due to water vapor and atmospheric liquid water than those from Ku-band altimeters. An attenuation algorithm is provided, based on radar propagation theory, which is a function of atmospheric pressure, temperature, water vapor, and liquid water content. Because of the nature of the air–sea interactions between wind and surface gravity waves, the shorter wavelength Ka-band backscatter exhibits a different relationship with wind speed than at Ku band, particularly at moderate to high wind speeds. This paper presents a new one-dimensional wind speed model, as a function of backscatter only, and a two-dimensional model, as a function of backscatter and significant wave height, tuned to AltiKa's backscatter measurements. The performance of these new Ka-band altimeter wind speed models is assessed through validation with independent ocean buoy wind speeds. The results indicate wind measurement accuracy comparable to that observed at Ku band with only slightly elevated noise in the wind estimates.

1. Introduction

SARAL—the Satellite with ARgos and ALtiKa—is a cooperative mission between the Indian Space Research Organization (ISRO) and Centre National d'Études Spatiales (CNES). The satellite was launched from Satish Dhawan Space Centre at 1231 UTC 25 February 2013 into a 35-day repeat orbit with a 99.85° inclination. The payload includes AltiKa, the first Ka-band radar altimeter to be flown in space, operating at 35.75 GHz, and a two-channel microwave radiometer operating at 23.8 and 37.0 GHz. The primary frequency for previous satellite radar altimeters has been at Ku band: 13.5–13.8 GHz. There are several advantages for Ka-band altimetry: smaller antenna, reduced sensitivity to ionospheric path delay, and higher along-track spatial resolution with lower range noise. However, there is one serious drawback: increased sensitivity to water vapor and liquid water in the atmosphere. At Ka band there is more attenuation of the radar signal from moisture than at Ku band, with the potential for significant data loss in rainy areas.

Sea surface height is the primary measurement from AltiKa, but estimates of ocean surface wind speed represent an important secondary measurement for operational maritime monitoring. Although altimeters do not provide wind direction (like scatterometers), their

Corresponding author address: John Lillibridge, NOAA/NESDIS/STAR, E/RA31, 5830 University Research Ct. 5344, College Park, MD 20740-3818.
E-mail: john.lillibridge@noaa.gov

DOI: 10.1175/JTECH-D-13-00167.1

wind speed estimates are an invaluable tool that is used for atmospheric model verification. This requires that attenuation effects are properly accounted for, and that an accurate wind speed model is used to estimate wind speed from backscatter.

The SARAL project began providing data within a few weeks of launch. Although the data quality was quite good, there were two significant issues requiring attention: 1) an estimate of backscatter attenuation due to the atmosphere was not yet provided, and 2) wind speeds were calculated using a wind speed model designed for Ku band. Because of the lack of attenuation corrections, the Ka-band backscatter is underestimated by 1 dB on average, with larger errors in rainy regions. Since there are no plans for an absolute backscatter calibration, once the attenuation effects have been corrected, the values are suitable for determination of wind speed. In section 2 we provide algorithms to compute the attenuation using atmospheric model inputs.

Using a Ku-band wind speed model with Ka-band backscatter results in large and systematic errors in global wind speed estimates. Abdalla (2014) provides one method to obtain reasonable wind speeds from AltiKa by modifying the backscatter values so the existing Ku-band wind speed model can be used. In section 3 we develop another approach, where the backscatter data are corrected for atmospheric attenuation but are unaltered otherwise. A new wind speed model is developed, using the same formalism, with coefficients tuned to AltiKa's backscatter. In section 4 we develop a two-dimensional model where wind speed is a function of backscatter and significant wave height (SWH). The final section assesses the performance of these one- and two-dimensional wind speed models using ocean buoy data and then summarizes our results.

2. A physically based attenuation model at Ka band

Atmospheric attenuation of the radar signal is more pronounced at Ka band than at Ku band. Consideration must be given to three components: attenuation due to oxygen molecules (dry atmosphere), water vapor molecules (wet atmosphere), and water droplets/rain (cloud liquid water).

To compute Ka-band attenuation, we exploit algorithms developed by the International Telecommunication Union (2012a,b) based on physical models of radar propagation through the atmosphere. Specifically, recommendation P-676 "Attenuation by Atmospheric Gases" provides formulas for the dry and wet atmosphere components, and recommendation P-840 "Attenuation due to Clouds and Fog" for attenuation due to cloud liquid water.

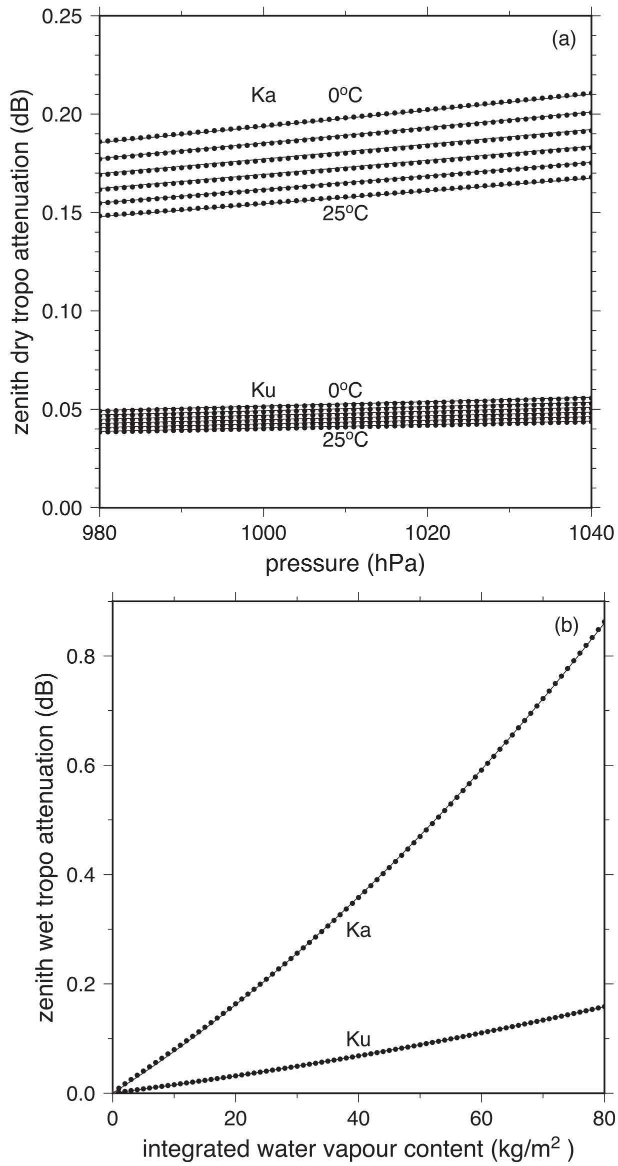

FIG. 1. Variations in backscatter attenuation in the Ku and Ka bands as a function of (a) pressure and temperature and (b) water vapor content.

These algorithms are functions of four two-dimensional (surface or total atmosphere) meteorological parameters: sea level pressure, near-surface atmospheric temperature, total precipitable water, and integrated cloud liquid water. We utilize the National Oceanic and Atmospheric Administration (NOAA)'s Global Forecast System (GFS) atmospheric model for all four input parameters.

The one-way Ka- and Ku-band dry atmosphere attenuation is empirically fit with a linear function of pressure and temperature as shown in Fig. 1a:

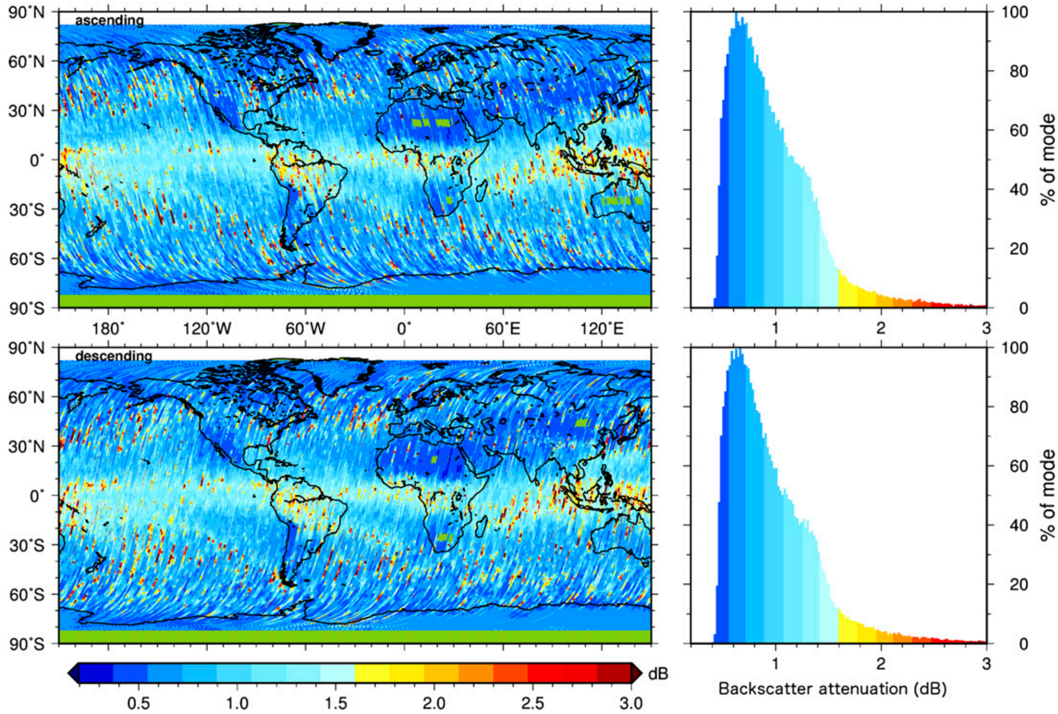

FIG. 2. Global distribution of two-way radar attenuation during cycle 1 of SARAL (14 Mar–18 Apr 2013). (left) (top) Ascending and (bottom) descending tracks. Histograms of (right) (top) ascending and (bottom) descending measurements.

$$\Delta\sigma^o_{\text{dry}} = \begin{cases} 0.094 - 0.177p' - 0.145t' + 0.274p't' & \text{for} \quad \text{Ku band} \\ 0.310 - 0.593p' - 0.499t' + 0.956p't' & \text{for} \quad \text{Ka band} \end{cases}, \tag{1}$$

where

$$\begin{aligned} p' &= p/1013 \quad & p &= \text{pressure in hPa} \\ t' &= 288.15/t \quad & t &= \text{temperature in K} \end{aligned}.$$

Although the pressure and temperature dependence of the dry attenuation is small at Ku band, it is important at Ka band.

The wet component of the one-way backscatter attenuation is fit as a quadratic function of total precipitable water (w, in kg m^{-2}) as shown in Fig. 1b:

$$\Delta\sigma^o_{\text{wet}} = \begin{cases} 1.45 \times 10^{-3}w + 0.66 \times 10^{-5}w^2 & \text{for} \quad \text{Ku band} \\ 7.21 \times 10^{-3}w + 4.43 \times 10^{-5}w^2 & \text{for} \quad \text{Ka band} \end{cases}. \tag{2}$$

The correction at Ka band is nearly 6 times as large as at Ku band.

The third component is a linear function of liquid cloud water (L, in kg m^{-2}):

$$\Delta\sigma^o_{\text{rain}} = \begin{cases} 0.169L & \text{for} \quad \text{Ku band} \\ 1.070L & \text{for} \quad \text{Ka band} \end{cases}. \tag{3}$$

This correction is about 7 times as large at Ka band as at Ku band.

The sum of dry, wet, and liquid water attenuation needs to be multiplied by 2 to account for the round-trip radar path, and is added to the uncorrected backscatter. This results in a shift of about +1 dB, equating to a 2.6 m s^{-1} decrease in wind speed, with the greatest effect in regions of high water vapor and cloud liquid water (Fig. 2). The uncertainty in attenuation correction from GFS model errors is estimated to be a few hundredths of a decibel. Given the wind speed relationship presented in the next section, this equates to uncertainties of less than 0.1 m s^{-1}. The attenuation corrections provided by the project team's neural network algorithm, using the onboard radiometer, can differ from our model estimates by several tenths of a decibel. These differences equate to 1–2 m s^{-1} differences in wind speed, and are highest in wet regions where this study's model predicts larger attenuation.

3. The one-dimensional wind speed model

After correcting for attenuation, we compute wind speed as a function of backscatter via a one-dimensional (1D) model. Abdalla (2014) provides a 1D model for AltiKa by adjusting the backscatter values so the mode of the probability density function agrees with typical Ku-band histograms. In this way the 1D Ku-band model used for the *European Remote Sensing Satellite-2* (*ERS-2*) and the *Environmental Satellite* (*Envisat*; Abdalla 2007, 2012) can be applied without modification.

Here we take a different approach: the backscatter values are corrected for attenuation only. The same 1D formulation is employed, but the model coefficients are adjusted rather than the backscatter values. The two-branch model combines a linear segment at low backscatter and an exponential segment at high backscatter, with a transition at the breakpoint σ_b, where the function and its first derivative are continuous. Fine-tuning is applied to provide the final ocean surface wind speed U_{10}, via Eqs. (4) and (5):

$$U_m = \begin{cases} \alpha - \beta\sigma^o & \text{if} \quad \sigma^o \le \sigma_b \\ \gamma \exp(-\delta\sigma^o) & \text{if} \quad \sigma^o > \sigma_b \end{cases} \tag{4}$$

$$U_{10} = U_m + 1.4U_m^{0.096}\exp(-0.32U_m^{1.096}). \tag{5}$$

All available data from AltiKa cycle 3, 23 May–27 June 2013, were analyzed. Data from cycles 0–2 were used to assess the quality of the model fit. Non-ocean data and records with the ice flag set were discarded. Any records with range standard deviation (SD) above 0.25 m or SWH SD above 1 m were also rejected. Coincident European Centre for Medium-Range Weather Forecasts (ECMWF) wind speeds were fit as a function of attenuation-corrected backscatter as described in Abdalla (2007, 2012). The distribution of data points in backscatter/wind speed space is shown in Fig. 3a, overlaid by a solid line showing the 1D wind speed model given by Eqs. (4) and (5) with

$$\begin{aligned} &\alpha = 34.2 \quad \beta = 2.48 \quad \sigma_b = 11.4 \\ &\gamma = 720 \quad \delta = 0.42 \end{aligned} \tag{6}$$

As expected from theory, the value of 2.48 for β is notably smaller for Ka band than the value of 3.6 for Ku band. The Abdalla (2007, 2012) Ku-band model is shown by the dashed line in Fig. 3a. This difference in slope is the reason that wind speeds currently in the product are unusable: the RMS error is around 13 m s^{-1}, which is 1.7 times the mean wind speed.

Figure 3b provides a scatterplot of the relationship between the 1D model wind speeds (y axis) and the ECMWF model wind speeds (x axis) for all of cycles 0–3. The scatterplot shows significant variability with a standard deviation of differences (SDD) of 1.41 m s^{-1} and a scatter index (defined as the SDD normalized by the mean ECMWF wind speed) of 18.0%. By comparison, the *Jason-2* Ku-band wind speed model exhibits an SDD of 1.16 m s^{-1} and a scatter index of 14.4%.

Figures 4a and 4b show the regional variations in bias and SDD, respectively, of the differences between the 1D model and ECMWF wind speeds. Bias values are within $\pm$2 m s^{-1} globally, with larger biases in the Southern Ocean, where ECMWF winds are less accurate due to fewer observations. The SDD values are less than 2 m s^{-1} over most of the global ocean, with a tendency toward higher values in wet regions.

4. The two-dimensional wind speed model

The one-dimensional model is a significant improvement over the wind speeds provided in the AltiKa products, with a slight improvement over the model proposed by Abdalla (2014). However, the scatter in altimeter versus ECMWF wind speeds, and previous experience with Ku-band data, suggests that a two-dimensional (2D) model as a function of backscatter and SWH should provide further improvement. The Jason missions adopted a 2D wind speed model (Gourrion et al. 2002; Collard 2005) to provide wind speed in their products. SWH as a second variable in the model serves as a proxy for long-wave roughness (unrelated to local winds). Although backscatter and SWH do not unambiguously distinguish between wind waves and long-period swell (Gourrion et al. 2002), we assess potential gains at Ka band from a 2D model.

ECMWF wind speeds for all Interim Geophysical Data Record (IGDR) data in AltiKa cycles 0–3, 12 March to 27 June 2013, were binned in backscatter–SWH space as seen in Fig. 5a. While at low backscatter there is significant variation from moderate to high wind speeds as a function of SWH, at higher backscatter this dependency is less apparent.

The population density of 1-Hz data points within each grid cell is shown in Fig. 5b. When the number of points per cell is low, variations in the mean values grow large, typically near the perimeter. To provide a complete grid beyond the region of high data density, we combine the 2D estimates in Fig. 5a with the 1D model, Eqs. (4)–(6), in Fig. 5c. The final "hybrid" model, Fig. 5d, is achieved by Gaussian smoothing the residuals between the 2D and 1D models, weighted by the population density in each cell, and adding back the 1D model. This method is similar to the construction of hybrid sea-state bias models with wind speed, rather

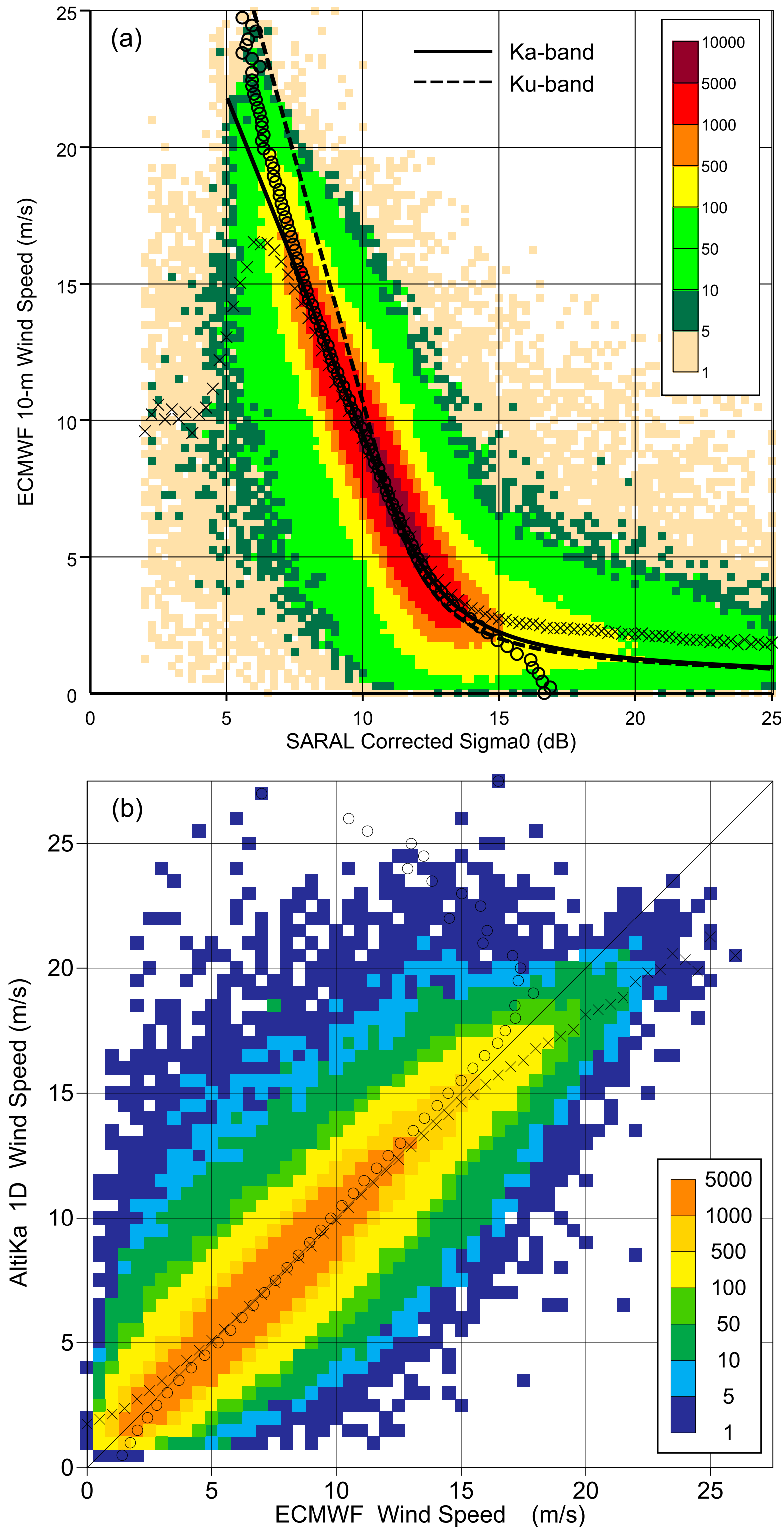

FIG. 3. Scatterplot of ECMWF wind speed (a) against AltiKa backscatter coefficient after attenuation correction and (b) against AltiKa wind speed as determined by the 1D model over the whole globe for SARAL repeat cycles 0–3. Solid line in (a) is for Eqs. (4)–(6). Color bar units are the number of observations per grid point on a logarithmic scale. The × symbols are the mean y values given x values, while the ○ symbols are vice versa. The Ku-band model from Abdalla (2012) is shown by the dashed line in (a).

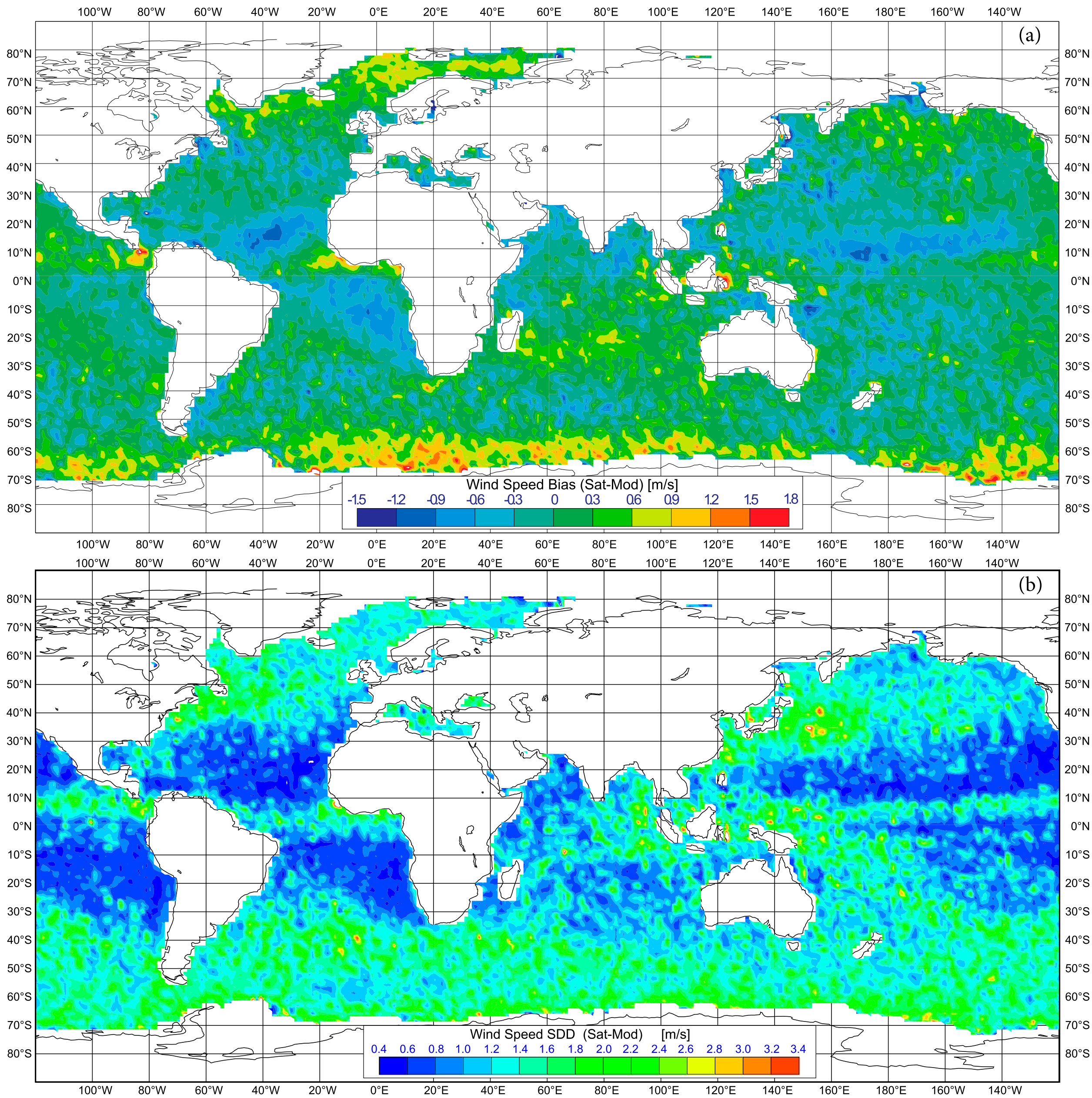

FIG. 4. Global map of (a) bias and (b) SDD between the 1D AltiKa wind speed model and ECMWF model winds.

than sea surface height, as the dependent variable (Vandemark et al. 2002; Scharroo and Lillibridge 2005).

The main differences between the 1D and 2D models are at low backscatter. When both backscatter and SWH are low, the 2D model yields significantly lower wind speeds than the 1D model. This is likely due to a correlation between SWH and backscatter during the radar echo ‘‘retracking’’ when the waveform is corrupted in rainy regions. More stringent editing of the original data could minimize this apparent artifact. At low backscatter, but high SWH, the 2D model predicts higher wind speeds than the 1D model. Both regimes have a low population density and are therefore downweighted in the final model. The 2D model presented here, which would be implemented as a simple lookup table, is viewed as an initial attempt. We expect further improvement with additional data as the mission lengthens, and the use of scatterometer winds in lieu of ECMWF values.

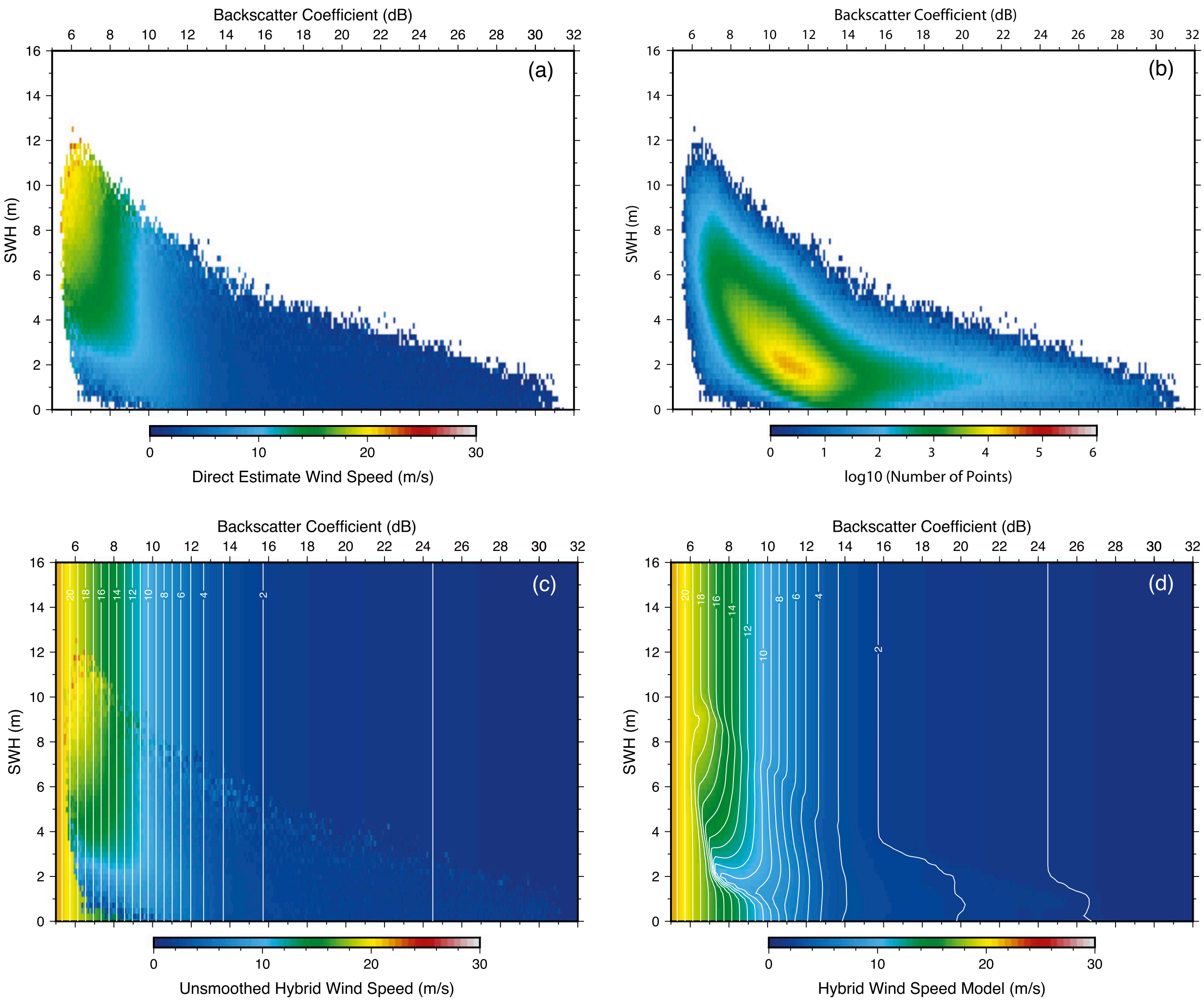

FIG. 5. Results from the 2D wind speed model: (a) ECMWF wind speed binned as a function of backscatter and significant wave height. (b) Number of observations per bin. (c) Binned values plotted over a background of the 1D model. (d) Hybrid solution, merging the binned estimate with the 1D model.

5. Validation and discussion

Investigations evaluating backscatter versus wind speed (e.g., Jackson et al. 1992; Liu et al. 2000; Vandemark et al. 2004) predict that differences between Ka and Ku bands are expected. Using optical techniques, Cox and Munk (1954) were able to establish a relationship between wind speed and ocean surface mean square slope (MSS). Assuming a quasi-specular reflection backscatter is inversely proportional to MSS, which can be divided into two components: one due to gravity waves and the other due to centimeter-scale gravity–capillary waves. For a one-dimensional wave spectrum $F(k)$ as a function of wavenumber k,

$$\mathrm{MSS} = \int_0^\infty F(k)k^2\,dk. \tag{7}$$

Altimeter backscatter changes can be attributed to changes across all roughness scales longer than roughly 3 times the wavelength (about 66 mm for Ku, about 24 mm for Ka), effectively limiting the wavenumber integration in Eq. (7) (Brown 1979). Thus, the higher-frequency Ka-band backscatter will respond to more of the small-scale wave spectrum. Since these shorter gravity–capillary waves are more responsive to wind, the Ka-band backscatter will exhibit a stronger wind speed dependence—hence, a smaller β value in Eq. (4)—than at Ku band. For low wind speeds, the longer gravity waves contribute significantly to the total surface roughness and the Ku–Ka-band backscatter differences are less apparent.

We assess the performance of the 1D and 2D models via comparisons with collocated wind speeds from ocean buoys (Bidlot et al. 2002). All collocations from cycles

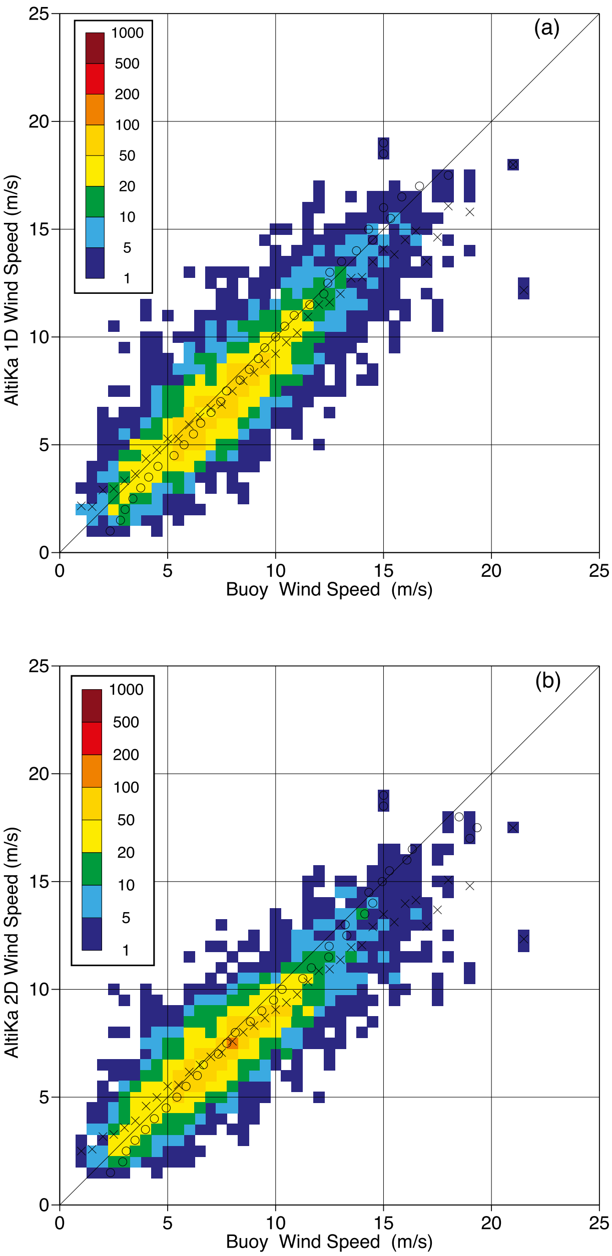

FIG. 6. Scatterplots of buoy wind speeds vs (a) 1D model and (b) 2D hybrid model wind speeds. Color bar units are number of observations per grid point, on a logarithmic scale. The X symbols are the mean *y* values given *x* values, while the ○ symbols are vice versa. The same number of observations based on collocations of buoy and model data were used in both panels.

0 to 3 were analyzed. With less than 5 months of data, and locations biased to the Northern Hemisphere, this does not sample all possible wind–wave conditions. AltiKa model winds (averaged over 11 s or 80 km) were collocated with buoy winds (averaged over 5 h) for the 1D and 2D models, shown in Figs. 6a and 6b, respectively. The 1D model regression lies closer to the 45° bisector, since the 2D model overestimates low winds and underestimates high winds. Both models have almost the same bias, about $-0.4\,\mathrm{m\,s^{-1}}$, compared to buoys. The 2D model has a slightly lower SDD of $1.46\,\mathrm{m\,s^{-1}}$ compared to $1.48\,\mathrm{m\,s^{-1}}$ for the 1D model. The Ka-band SDD is somewhat higher than for Ku-band altimeters, which are typically less than $1.2\,\mathrm{m\,s^{-1}}$ (e.g., Abdalla et al. 2011).

Based on these results, the 1D and 2D models are comparable in performance. Further analysis and development of the 2D model, primarily with collocated scatterometer winds, could result in a model that ultimately outperforms the 1D model.

These early mission results show that Ka-band altimetry can provide ocean surface wind speed estimates with only moderately higher uncertainty than those obtained from Ku-band altimeters. With additional observations, the 1D model coefficients could be refined, but the 1D model presented here, based on one 35-day cycle, provides robust results over the first 120 days of AltiKa measurements. The project team has endorsed the 1D model, and wind speed values provided in the official products will be based on it beginning in early 2014. Regardless of which model is utilized, the Ka-band backscatter measurements need to be corrected for attenuation effects. The algorithms in section 2 provide a means to compute this correction using global weather model grids.

Acknowledgments. The authors thank Hui Feng for his verification analysis using NDBC buoys, and Natalia Galin for her assistance with the attenuation model. The views, opinions, and findings in this manuscript are those of the authors, and they should not be construed as an official NOAA or U.S. government position, policy, or decision.

REFERENCES

Abdalla, S., 2007: Ku-band radar altimeter surface wind speed algorithm. *Proceedings of the Envisat Symposium 2007,* H. Lacoste and L. Ouwehand, Eds., European Space Agency Publ. ESA SP-636, 463250. [Available online at https://earth.esa.int/workshops/envisatsymposium/proceedings/sessions/3E4/463250sa.pdf.]

——, 2012: Ku-band radar altimeter surface wind speed algorithm. *Mar. Geod.,* **35** (Suppl.), 276–298, doi:10.1080/01490419.2012.718676.

——, 2014: Calibration of SARAL/AltiKa wind speed. *IEEE Geosci. Remote Sens. Lett.,* **11,** 1121–1123, doi:10.1109/LGRS.2013.2287805.

——, P. A. E. M. Janssen, and J.-R. Bidlot, 2011: Altimeter near real time wind and wave products: Random error estimation. *Mar. Geod.,* **34,** 393–406, doi:10.1080/01490419.2011.585113.

Bidlot, J.-R., D. J. Holmes, P. A. Wittmann, R. Lalbeharry, and H. S. Chen, 2002: Intercomparison of the performance of the operational wave forecasting systems with buoy data. *Wea. Forecasting,* **17,** 287–310, doi:10.1175/1520-0434(2002)017<0287:IOTPOO>2.0.CO;2.

Brown, G. S., 1979: Estimation of surface wind speeds using satellite-borne radar measurements at normal incidence. *J. Geophys. Res.,* **84,** 3974–3978, doi:10.1029/JB084iB08p03974.

Collard, F., 2005: Algorithmes de vent et période moyenne des vagues JASON à base de réseaux de neurons. BO-021-CLS-0407-RF, Boost Technologies, 33 pp.

Cox, C., and W. Munk, 1954: Measurement of the roughness of the sea surface from photographs of the sun's glitter. *J. Opt. Soc. Amer.,* **44,** 838–850, doi:10.1364/JOSA.44.000838.

Gourrion, J., D. Vandemark, S. Bailey, B. Chapron, G. P. Gommenginger, P. G. Challenor, and M. A. Srokosz, 2002: A two-parameter wind speed algorithm for Ku-band altimeters. *J. Atmos. Oceanic Technol.,* **19,** 2030–2048, doi:10.1175/1520-0426(2002)019<2030:ATPWSA>2.0.CO;2.

International Telecommunications Union, 2012a: Recommendation ITU-R P.676-9: Attenuation by atmospheric gases. P Series, Radiowave Propagation, 24 pp. [Available online at http://www.itu.int/dms_pubrec/itu-r/rec/p/R-REC-P.676-9-201202-S!!PDF-E.pdf.]

——, 2012b: Recommendation ITU-R P.840-5: Attenuation due to clouds and fog. P Series, Radiowave Propagation, 10 pp. [Available online at http://www.itu.int/dms_pubrec/itu-r/rec/p/R-REC-P.840-5-201202-S!!PDF-E.pdf.]

Jackson, F. C., W. T. Walton, D. E. Hines, B. A. Walter, and C. Y. Peng, 1992: Sea surface mean square slope from K_u-band backscatter data. *J. Geophys. Res.,* **97,** 11 411–11 427, doi:10.1029/92JC00766.

Liu, Y., M.-Y. Su, X.-H. Yan, and W. T. Liu, 2000: The mean-square slope of ocean surface waves and its effects on radar backscatter. *J. Atmos. Oceanic Technol.,* **17,** 1092–1105, doi:10.1175/1520-0426(2000)017<1092:TMSSOO>2.0.CO;2.

Scharroo, R., and J. Lillibridge, 2005: Non-parametric sea-state bias models and their relevance to sea level change studies. *Proceedings of the 2004 Envisat and ERS Symposium,* H. Lacoste and L. Ouwehand, Eds., European Space Agency Publ. ESA SP-572, 2P05-1. [Available online at http://earth.esa.int/workshops/salzburg04/papers_posters/2P05_1_scharroo_198r.pdf.]

Vandemark, D., N. Tran, B. D. Beckley, B. Chapron, and P. Gaspar, 2002: Direct estimation of sea state impacts on radar altimeter sea level measurements. *Geophys. Res. Lett.,* **29,** 2148, doi:10.1029/2002GL015776.

——, B. Chapron, J. Sun, G. H. Crescenti, and H. C. Graber, 2004: Ocean wave slope observations using radar backscatter and laser altimeters. *J. Phys. Oceanogr.,* **34,** 2825–2842, doi:10.1175/JPO2663.1.